Optimization of Stiffness per Magnet Volume Ratio of Discrete and Continuous Halbach Type Permanent Magnetic Bearings

Edmund Marth*, Gerald Jungmayr, Martin Panholzer, Wolfgang Amrhein
Institute of Electrical Drives and Power Electronics
Johannes Kepler University Linz
Shareholder of the ACCM GmbH
Linz, Austria

Abstract

To optimize stiffness per magnet volume ratio, whichs major intentions are to reduce the costs and to preserve material resources, an energy based analytical calculation method of the radial stiffness for permanent magnetic bearings with arbitrary magnetization is introduced. To simplify the calculations the stiffness is calculated from a planar model, what means that the annular ring magnets are treated as infinitely long parallel bars. The error made by neglecting the curvature effect is investigated and shows to be negligible for reasonable designs. Using this calculation method, optimal geometries for permanent magnetic ring bearings with Halbach type magnetization are presented. Thereby, discrete Halbach stacking, i.e. several stacked rings with rotating magnetization from axial to radial and so on, and continuous Halbach magnetization, i.e. one magnet that is magnetized sinusoidal, is distinguished. To show the possible improvement of stiffness per magnet volume ratio, also the characterizing values for standard single ring bearings and standard stacked structures are calculated.

1 Introduction

Besides the very high robustness of passive permanent magnetic ring bearings, the relatively low costs compared to active magnetic bearing units was one of the main advantages until a few years ago. Although the rare earth prices are decreasing since the past half year, the global trend of the rare earth market, with raw material prices rising considerably in the recent past, tends to overcome this. To keep the total costs of systems including passive magnetic bearings low, the objective of optimal stiffness per magnet volume ratio has taken on new significance. Considering a single ring bearing, this objective is a function of only two major dimensionless parameters, as shown by Lang [1]. These parameters are the ratios a/h and b/h with the magnets cross section dimensions a and b and the air gap width h. A third characterizing parameter, depending on the mean air gap radius r_h, has only a minor relevance, what will also be shown in the paper. But this single ring optimum can be improved by more than 40% when stacked structures with alternating magnetization of the rings are used. While Lang and others showed this in a generally valid form, Yonnet showed for a special case, that the ratio of stiffness per magnet volume can be raised even more when using a, as Yonnet called it, “rotating magnetization”, i.e. the direction of magnetization varies with 90 degree steps, from axial to radial and so on [2]. A generalized discussion of such stacked Halbach-type structures with universally valid results, based on dimensionless parameters, will be presented in this paper. Following the refinement prozess of the disretization steps of the magnetizations rotation, from 180° (standard stacking) to 90° (Halbach stacking) one comes to a continuous rotation of the magnetization, as e.g. presented in [3]. In order to find an analytical solution for this problem, a calculation technique based on the interaction energy of magnetic dipoles is introduced.

*edmund.marth@jku.at, Altenbergerstrasse 69, 4040 Linz, Austria, Phone/Fax: +43 732 2468 6432/6423

2 Stiffness calculation of magnets with an arbitrary magnetization distribution

The analytical calculation of forces and stiffness of passive permanent magnetic bearings has been described in numerous publications. Based on the "source" of magnetic induction different calculation approaches can be found. The vast majority utilizes magnetic surface charges to model uniformly axial or radial magnetized rings [4–7]. What is the more adequate formulation from a physical point of view is the one using so called current sheets. This approach was used by Lang for axial magnetized rings [8]. Both methods are basically founded on three dimensional magnetic (fictive) charge- or current density distributions respectively, which can be reduced to surface charges or laminar current sheets for the case of homogeneous magnetization directions. For an arbitrary, i.e. not uniform, magnetization the divergence or rotation of the describing charge- or current density distribution has to be calculated respectively, what would lead to a more complex calculation. An interesting approach was introduced by Yonnet, starting one abstraction level above the charge– or current model. In [9] the calculation of induction, forces and stiffness is based on elementary magnetic dipoles. The advantage thereby is, that the magnetization function $\mathbf{M}$ is a direct parameter and no rotation, divergence or other laminar surrogate parameters have to be calculated, regardless of the function of the magnetization distribution.

Beside the different modeling concepts concerning the "source" of magnetic induction, two different geometrical representations are widely found – the exact one considering the rotational symmetry of the rings, e.g. [8], and an approximation, where the induction is calculated from an infinitely long rod. The curvature effect is thus neglected, allowing a simplified calculation [9], [4].

The calculation technique used in this publication is based on [9], with elementary magnetic dipoles describing the overall magnetization of the bearing. Furthermore, the approximate plane model will be used describing the annular devices, whereby an error analysis concerning the plane model representation of the magnet rings is presented in a following section.

2.1 The planar model

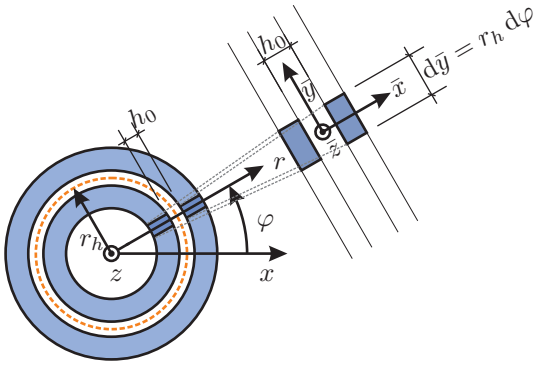

Figure 1: Modeling of an arc segment as a planar line element.

To simplify the force and stiffness calculation of passive magnetic bearings the point wise repulsive radial force $\mathrm{d}F_r(\varphi)$ acting along the circumference of the bearings rings is assumed to be

$$\mathrm{d}F_r(\varphi) = -\int_{\infty}^{h(\varphi)} \bar{k}_{\bar{x}}(\bar{x})\,\mathrm{d}\bar{x}\ , \tag{1}$$

where $\bar{k}_{\bar{x}}$ is the stiffness per length of two parallel magnets as zoomed out in Figure 1. The total radial force

$F(\varphi)$ acting on a ring, lets say in the $\varphi = 0°$ direction, thus is

$$F(0) = \int_0^{2\pi} \mathrm{d}F_r(\varphi)\cos(\varphi) r_h \,\mathrm{d}\varphi = -\int_0^{2\pi}\int_\infty^{h(\varphi)} \bar{k}_{\bar{x}}(\bar{x})\,\mathrm{d}\bar{x}\cdot\cos(\varphi) r_h \,\mathrm{d}\varphi \tag{2}$$

where $h(\varphi)$ in its general form is defined as

$$h(\varphi) = h_0 + (e + h_\Delta)\cos\varphi \ . \tag{3}$$

In (3) h_0 denotes the nominal air gap width of a concentric configuration and e describes an eccentricity of e.g. the inner ring in the $\varphi = 0°$ direction. With the additional parameter h_Δ, describing small free movements again in the $\varphi = 0°$ direction, the radial stiffness k_r with a certain eccentricity e can be calculated by $k_r = -\frac{\mathrm{d}F}{\mathrm{d}h_\Delta}$ using the Leibniz integral rule.

$$k = -\frac{\mathrm{d}F}{\mathrm{d}h_\Delta} = \int_0^{2\pi} \bar{k}_{\bar{x}}\Big(h(\varphi)\Big)\cos^2(\varphi) r_h \,\mathrm{d}\varphi \tag{4}$$

When looking at the linearized stiffness ($h_\Delta \to 0$) at concentric position ($e = 0$) the value $h(\varphi) = h_0 = \text{const.}$ and thus (4) leads to

$$k_r = \bar{k}_{\bar{x}}(h_0)\pi r_h \ . \tag{5}$$

The actual ring stiffness is equal the stiffness of the planar model with half the length of the rings perimeter. The total axial stiffness can be found straight forward to be the stiffness per length multiplied with the rings total perimeter,

$$k_z = \bar{k}_{\bar{z}}(h_0) 2\pi r_h \ . \tag{6}$$

How to calculate $\bar{k}$ will be shown later on in the paper.

2.2 Error of the planar model

Basically, the planar model is exact for the case of $r_h \to \infty$. This is because the curvature effect vanishes for this theoretical case and just this mentioned curvature effect is neglected when modeling annular problems as planar configurations. However, in reality the curvature has a more or less influence on the stiffness value of passive magnetic bearings. How big this error is, will be shown in this section depending on all error relevant parameters.

At first two main arrangements of passive magnetic bearings have to be distinguished – attractive and repulsive configurations. In Figure 2 single ring radial bearings in repulsive and attractive configuration are

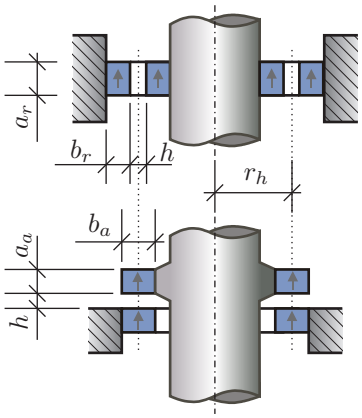

Figure 2: Passive magnetic single ring radial bearings stabilized by repulsive (upper configuration) and attractive (lower configuration) forces. With $a_r = b_a$ and $a_a = b_r$ (7) holds true (with same air gap dimension h for both configurations).

pictured. Based on the planar model it can be shown, that

$$\bar{k}_{r,rep} = f(a,b,h) \Leftrightarrow \bar{k}_{r,att} = f(b,a,h) \tag{7}$$

holds true [10]. Nevertheless, the error caused by the planar model is not the same for repulsive and attractive configurations, what in fact means that (7) is not exact for the real case. In Figs. 3 and 4 the error is shown for single ring bearings as function of the dimensionless parameters a/h, b/h and r_h/h for attractive and repulsive configurations respectively. When looking at the error plots of attractive configurations, Figure 3(a) and

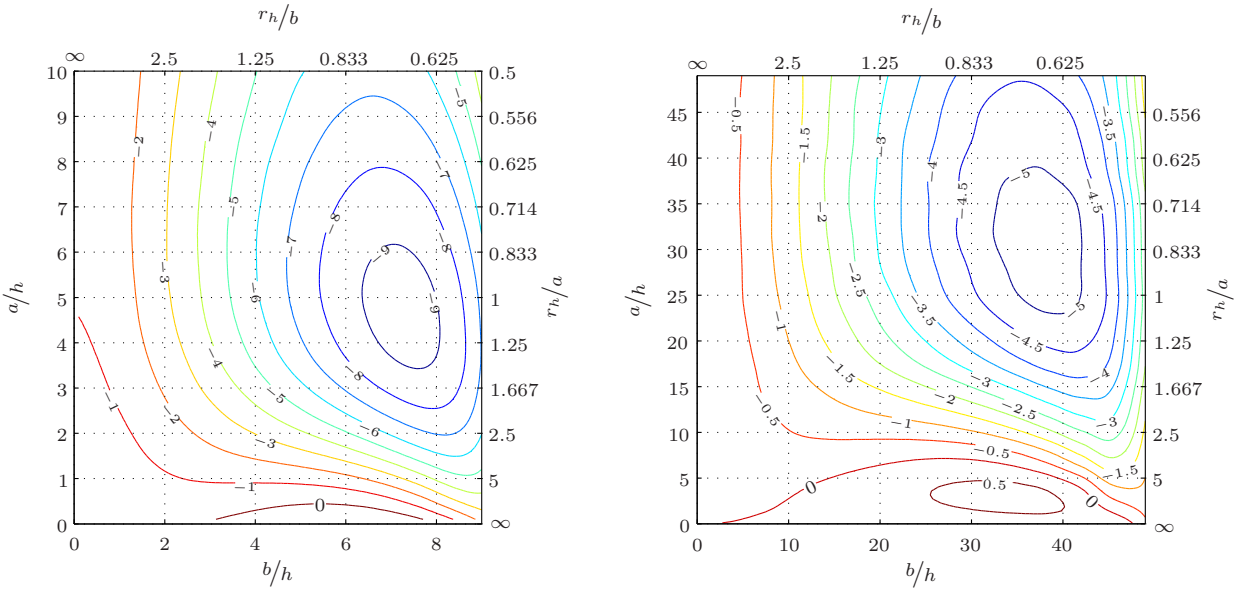

(a) $r_h/h = 5$ (b) $r_h/h = 25$

Figure 3: Relative error of the radial stiffness of attractive single ring bearings, calculated as $err = (k_{planar}/k_{rotsym} - 1) \cdot 100$. The exact solution k_{rotsym} was gained by the solutions given in [11]. The planar solution k_{planar} is derived from (5) and (20). The error is shown for different values of r_h/h.

3(b), one can see that the qualitative error as function of the parameters r_h/a and r_h/b is only dependent on the parameter r_h/h. The maximum error always lies around $r_h/a \approx 1$ and $r_h/b \approx 0.65$ and is below 10% even for very small vaues of r_h/h. With rising values of r_h/h the error gets significantly smaller. When comparing Figs. 3(a) and 3(b), take care of the different values of the a/h and b/h axes, e.g. for a bearing with a magnets cross sections of $a/h = 5$ and $b/h = 7$ the error for $r_h/h = 5$ is more than 9%, with $r_h/h = 25$ a bearing with the same cross sections and airgap (only with a bigger radius) has an error around 0.2%.

Later on it will be shown, that for a reasonable stiffness per magnet volume ratio the value of the parameters a/h and b/h should be below 3, whereby the error caused by the planar model is always smaller than 3% with $r_h/h \geq 5$ for an attractive type single ring bearing.

Even the, lets say, worst case error of 3% for attractive single ring bearings is quite good, the error for repulsive configurations is much smaller, as can be seen from the figures 4(a) and 4(b). For reasonable cross section geometries – as mentioned before – the error can be said to be below 1% for $r_h/h \geq 5$ and is rapidley shrinking further for growing values of r_h/h.

Conclusion: What can be seen is, that the error caused by the planar model is very small and might be negligible when thinking about fabrication tolerances of the used permanent magnets or inaccuracies when assembling the bearing system.

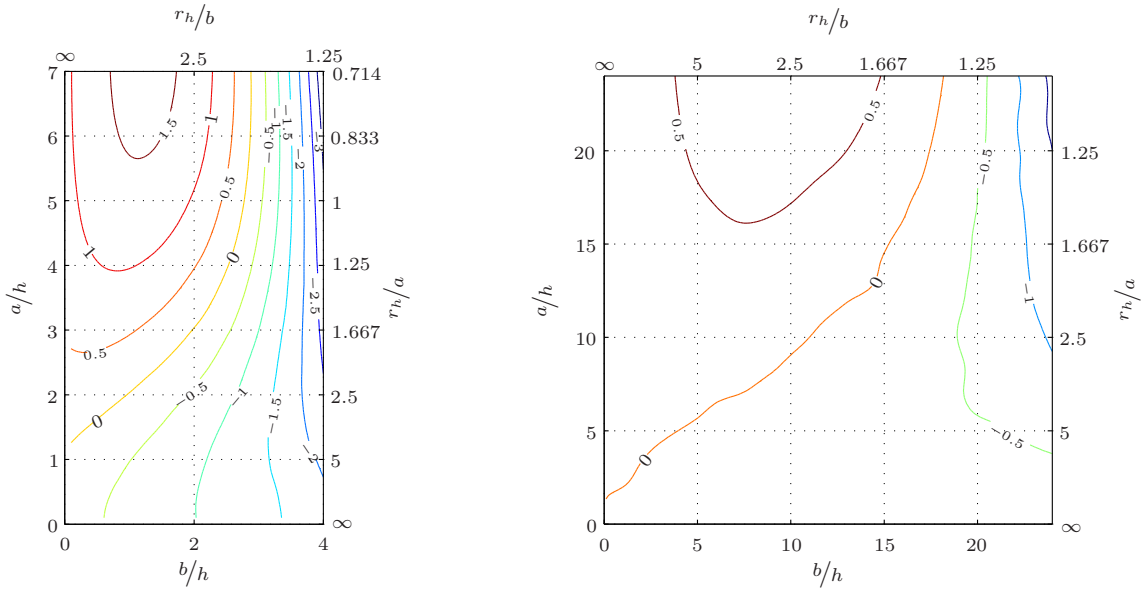

(a) $r_h/h = 5$ (b) $r_h/h = 25$

Figure 4: Relative error as shown in Figure 3 but for repulsive configurations.

2.3 Stiffness calculation based on the planar model

2.3.1 Induction of a line dipole

The induction caused by a magnetic dipole with the dipole moment $\mathbf{m}$ can be calculated for the tree-dimensional case by [12]

$$\mathbf{B}(\mathbf{r}) = \frac{\mu_0}{4\pi} \frac{3\mathbf{r}(\mathbf{m}\cdot\mathbf{r}) - |\mathbf{r}|^2\mathbf{m}}{|\mathbf{r}|^5} \,. \tag{8}$$

For the plane model, a magnetic dipole per length $\bar{\mathbf{m}}$ is defined. In Figure 5 two such line dipoles, representing the two rings, are pictured. For the plane case, an equivalent formulation to (8) can be found, describing

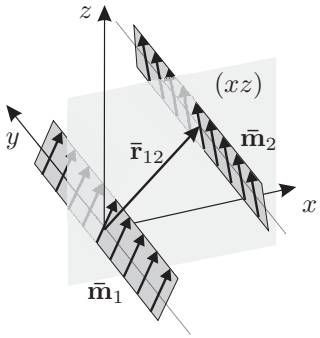

Figure 5: Two line dipoles in the (xz) – plane

the in plane induction $\bar{\mathbf{B}}$ caused by the line dipole $\bar{\mathbf{m}}$ at distance $\bar{\mathbf{r}}$.

$$\bar{\mathbf{B}}(\bar{\mathbf{r}}) = \frac{\mu_0}{2\pi} \frac{2\bar{\mathbf{r}}(\bar{\mathbf{m}}\cdot\bar{\mathbf{r}}) - |\bar{\mathbf{r}}|^2\bar{\mathbf{m}}}{|\bar{\mathbf{r}}|^4} \tag{9}$$

Thereby all vectors labeled by a bar $\bar{(\cdot)}$ are defined in the (xz) - plane.

$$\bar{\mathbf{r}} = \begin{pmatrix} x \\ z \end{pmatrix} \ , \quad \bar{\mathbf{m}} = \begin{pmatrix} m_x \\ m_z \end{pmatrix} \ , \quad \bar{\mathbf{B}} = \begin{pmatrix} B_x \\ B_z \end{pmatrix} \tag{10}$$

2.3.2 Force of a line dipole in an external B– field

Based on the spatial equation for the force exerted on a magnetic dipole by an external induction field [12] $\mathbf{F} = \nabla(\mathbf{m} \cdot \mathbf{B})$ again a two dimensional formulation can be written

$$\bar{\mathbf{F}} = \bar{\nabla}(\bar{\mathbf{m}} \cdot \bar{\mathbf{B}}) \ , \tag{11}$$

where $\bar{\nabla}$ is the gradient in the $x - z$ plane. Looking at Figure 5, with (11) the force acting on line dipole $\bar{\mathbf{m}}_2$ within the magnetic field caused by $\bar{\mathbf{m}}_1$ could be calculated.

2.3.3 Interaction energy of two line dipoles

The energy of a magnetic dipole within an external **B**- field can be gained for the three dimensional case from $U = -\int \mathbf{F}\,\mathrm{d}\mathbf{r} = -\int \nabla(\mathbf{m} \cdot \mathbf{B})\,\mathrm{d}\mathbf{r} = -\mathbf{m} \cdot \mathbf{B}$. The equivalent formulation in two dimensions is thus

$$\bar{U} = -\bar{\mathbf{m}} \cdot \bar{\mathbf{B}} \ . \tag{12}$$

The interaction energy between a dipole $\bar{\mathbf{m}}_1$ and a second one $\bar{\mathbf{m}}_2$ can now be calculated by evaluating the induction caused by $\bar{\mathbf{m}}_1$ at the place of $\bar{\mathbf{m}}_2$ via (9) multiplied by $\bar{\mathbf{m}}_2$.

$$\bar{U} = -\bar{\mathbf{m}}_2 \cdot \bar{\mathbf{B}}_1(\bar{\mathbf{r}}_{12}) = -\frac{\mu_0}{2\pi}\left(\frac{2(\bar{\mathbf{m}}_2 \cdot \bar{\mathbf{r}}_{12})(\bar{\mathbf{m}}_1 \cdot \bar{\mathbf{r}}_{12})}{|\bar{\mathbf{r}}_{12}|^4} - \frac{\bar{\mathbf{m}}_1 \cdot \bar{\mathbf{m}}_2}{|\bar{\mathbf{r}}_{12}|^2}\right) \tag{13}$$

2.3.4 Stiffness calculation based on the interaction energy of line dipoles under consideration of real cross section dimensions

The previous derivation of the interaction energy is related to elementary dipoles. But if real magnets with e.g. rectangular cross section are represented as single dipoles, the distance between the two magnets has to be at least larger than the cross section dimensions to get a feasible result. This was assumed in [9] but is clearly not suitable for the calculation of well designed passive magnetic bearings, where a high stiffness value is strongly related to a small air gap dimension.

To overcome this problem, a magnet can be seen as a sum of small elementary dipoles $\mathrm{d}\mathbf{m}$ and the interaction between each dipole of both magnets is calculated and summed up to get the total energy. Shrinking the discretization size toward zero, the density of the magnetic dipole moment, the magnetization $\mathbf{M}$ defined via $\mathrm{d}\mathbf{m} = \mathbf{M}\,\mathrm{d}V$ or for the planar problem

$$\mathrm{d}\bar{\mathbf{m}} = \bar{\mathbf{M}}\,\mathrm{d}A \ , \tag{14}$$

can be introduced. The result gained by this method is also valid for small air gap dimensions. The total interaction energy per length of two permanent magnets as pictured in Figure 6 can thus be calculated from (13) using (14).

$$\bar{U} = -\frac{\mu_0}{2\pi}\iint\limits_{A_1 A_2}\left(\frac{2(\bar{\mathbf{M}}_2(\bar{\mathbf{r}}_2) \cdot \bar{\mathbf{r}}_{12})(\bar{\mathbf{M}}_1(\bar{\mathbf{r}}_1) \cdot \bar{\mathbf{r}}_{12})}{\bar{r}_{12}^4} - \frac{\bar{\mathbf{M}}_1(\bar{\mathbf{r}}_1) \cdot \bar{\mathbf{M}}_2(\bar{\mathbf{r}}_2)}{\bar{r}_{12}^2}\right)\mathrm{d}A_2\,\mathrm{d}A_1 \tag{15}$$

Equation (15) can now be used for arbitrary configurations with appropriate parametrization of $\bar{\mathbf{M}}_1$ and $\bar{\mathbf{M}}_2$. The acting forces can be calculated by

$$\bar{\mathbf{F}} = -\bar{\nabla}_0 \bar{U} \tag{16}$$

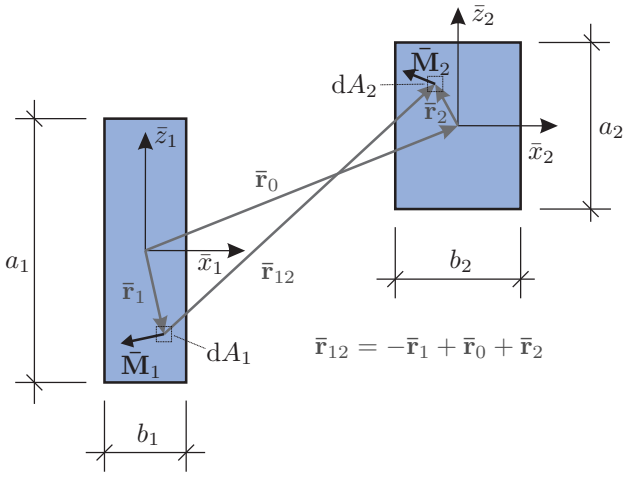

Figure 6: Cross sections of two magnetic rings with arbitrary magnetization functions $\bar{\mathbf{M}}_i(\mathbf{r}_i)$, $i \in \{1,\ 2\}$

where $\bar{\nabla}_0$ is the derivation with respect to $\bar{\mathbf{r}}_0$, compare Figure 6. With the general definition of the stiffness $k_x = -\partial F_x / \partial x$ it follows that

$$\bar{\mathbf{k}}_i = -\frac{\partial \bar{\mathbf{F}}_i}{\partial \bar{\mathbf{r}}_{0,i}} = \frac{\partial^2 \bar{U}}{\partial \bar{\mathbf{r}}_{0,i}^2} , \quad i \in \{x, z\} . \tag{17}$$

For various parametrizations of $\bar{\mathbf{M}}(\bar{\mathbf{r}})$ analytical solutions for $\bar{k}$ can be calculated. Finally, the total stiffness of the annular device can be calculated using (5) and (6).

One assumption that was used all the time during the derivation of the stiffness value was, that the relative permeability $\mu_r = 1$ for the magnet and all elements in the bearings vicinity. This is widely true for sintered NdFeB or SmCo magnets but might be a source of error when using ferrite magnets or polymer bonded magnets in general.

2.3.5 Stiffness per magnet volume

As can be seen from (5) and (6) the total ring stiffness is linearly proportional to the mean air gap radius r_h. As it is the goal to optimize the stiffness per magnet volume ratio, it is obvious that r_h cancels out when dividing by the rings volume, and the stiffness per length per magnet cross section area remains. To get rid of the influence of the remanence strength of the magnet on the optimization parameter, the reference pressure

$$\sigma_{ref} = \frac{B_r^2}{2\mu_0} \tag{18}$$

is introduced and finally making the whole expression dimensionless leads to

$$\bar{k}_r^A = \bar{k}_r \frac{h^2}{A \cdot \sigma_{ref}} . \tag{19}$$

The optimization parameter (19) is similar to the dimensionless parameter defined in [1] for the exact case considering the annular shape. With equal cross section dimensions for both rings the magnet area is defined as $A = 2ab$ for single ring bearings or $A = 2abn$ for stacked bearings with stacking number n, see Figure 9.

Clearly, $\bar{k}_r^A$ is not a stiffness per volume quantity, but represents a parameter which is proportional to the stiffness per magnet volume. Thus, the goal will be to maximize the normalized parameter $\bar{k}_r^A$.

3 From a single ring bearing to continuous rotating magnetization

All results presented in this section are derived by proper evaluation of (15) and (17). To show the possible improvement of stiffness to magnet volume ratio the known results concerning single ring bearings and multi ring bearings with alternating magnetization, [1], are recalculated using (19).

3.1 Single ring bearings

For single ring bearings as pictured in Figure 7 the stiffness per length evaluates to

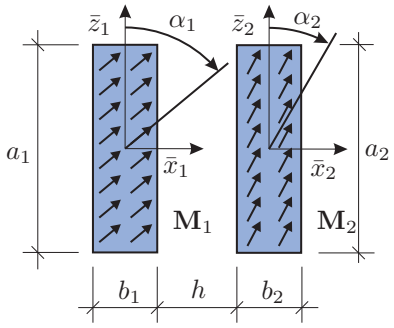

Figure 7: Homogeneous magnetization with arbitrary magnetization directions α_1 and α_2.

$$\bar{k}_r = \frac{B_r^2}{2\mu_0\pi}\cos(\alpha_1+\alpha_2)\cdot\left[2\ln\left(\frac{(b+h)^2}{a^2+(b+h)^2}\right)+\ln\left(\frac{(a^2+h^2)(a^2+(2b+h)^2)}{h^2(2b+h)^2}\right)\right] , \tag{20}$$

whereby

$$\bar{\mathbf{M}}_i = M_i\begin{bmatrix}\sin\alpha_i\\ \cos\alpha_i\end{bmatrix} \ , \ i\in\{1,2\} \tag{21}$$

and

$$a_1=a_2=a \ , \ b_1=b_2=b \ , \ z_0=0 \ , \ M_1=M_2=\frac{B_r}{\mu_0} \tag{22}$$

was used. z_0 describes the displacement between the two magnets in $\bar{z}$ direction, i.e. the z component of the $\bar{\mathbf{r}}_0$ vector of Figure 6.

Based on (20) some interesting facts should be mentioned. What is only valid for $z_0 = 0$ is, that the stiffness is maximal when $\alpha_1 = -\alpha_2$. That $\bar{k}_r$ is invariant against the sum $\alpha_1+\alpha_2$ holds true also for $z_0 \neq 0$. At last, a very interesting aspect of (20) is, that scaling all geometric parameters by a factor L,

$$(a,b,h)\rightarrow(L\cdot a, L\cdot b, L\cdot h) \tag{23}$$

has no influence on $\bar{k}_r$, since L cancels out in the $\ln(\cdot)$ terms. Thus, the optimal geometry can be described as function of the two already introduced parameters a/h and b/h. Optimizing for the dimensionless parameter (19) using (25) leads to a distinct maximum value of $\hat{\bar{k}}_r^A = 0.05893$ at $a = 1.01757\cdot h$ and $b = 0.669685\cdot h$. The optimization was done with the computer algebra program Mathematica©.

The sensitivity of the optimal parameters of a single ring bearing is shown in Figure 8. The dashed and dash-dotted lines denote the optimal b/h or a/h for given a/h or b/h respectively.

3.2 Standard stacking

With a generalized stiffness of a single ring bearing, similar to (20) but with arbitrary axial displacement of the two rings z_0,

$$\bar{k}_r(z_0,\alpha_\Sigma) \ , \quad \alpha_\Sigma=\alpha_1+\alpha_2$$

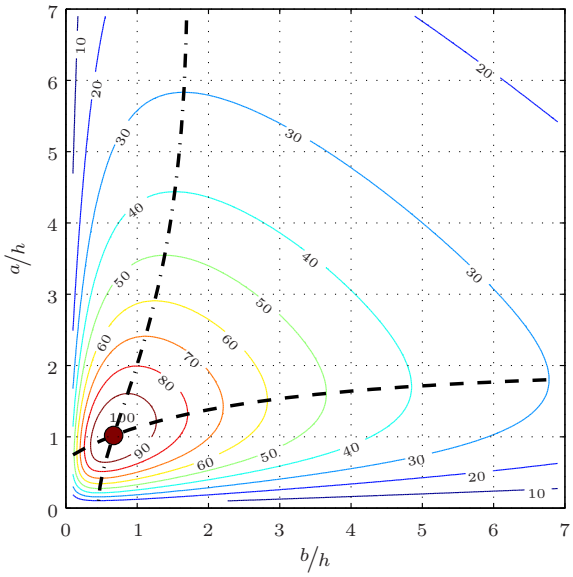

Figure 8: Normalized radial stiffness with respect to $\hat{\bar{k}}_r^A$ of a repulsive type single ring bearing and the dimensionless parameters $^a/_h$ and $^b/_h$ in %

the total stiffness of standard stacked multi ring bearings as pictured in Figure 9 can be calculated using

$$\bar{k}_r^n = n \cdot \bar{k}_r(0,0) + \sum_{i=1}^{n-1} 2 \cdot (n-i) \cdot \bar{k}_r(i \cdot a, -i \cdot \pi) \ . \tag{24}$$

The already mentioned invariance of $\bar{k}_r$ with respect to α_Σ is extensively used in (24). To calculate the

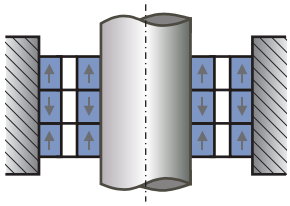

Figure 9: Stacked structure with alternating magnetization and $n = 3$.

normalized parameter $\bar{k}_r^A$, (24) is used for the parameter $\bar{k}_r$ in (19). As can be seen from Table 1, $\bar{k}_r^A$ can be improved up to 50% when using stacked structures in stead of single ring bearing configurations. A vivid explanation for this improvement is given by equation (24). The difference between n single ring bearings and a stacked structure is the sum- term, which represents the coupling between e.g. the first outer ring with the second inner ring and so on. The improvement values of Table 1, i.e its last column entries, are in

exact agreement with [13]. The sensitivity of a stacked bearing with five rings is shown in Figure 10.

stacking n	max parameters: norm. magnet height a/h	max parameters: norm. magnet width b/h	max. value $\hat{\bar{k}}_r^A$	increase compared to $n=1$ in %
1	1.018	0.670	0.05893	–
2	1.296	0.652	0.07793	32.3
3	1.447	0.643	0.08096	37.4
4	1.497	0.641	0.08300	40.8
5	1.522	0.640	0.08443	43.3
10	1.571	0.637	0.08734	48.2
20	1.592	0.637	0.08887	50.8

Table 1: Normalized, dimensionless radial stiffness for repulsive configurations with different numbers of stacked rings

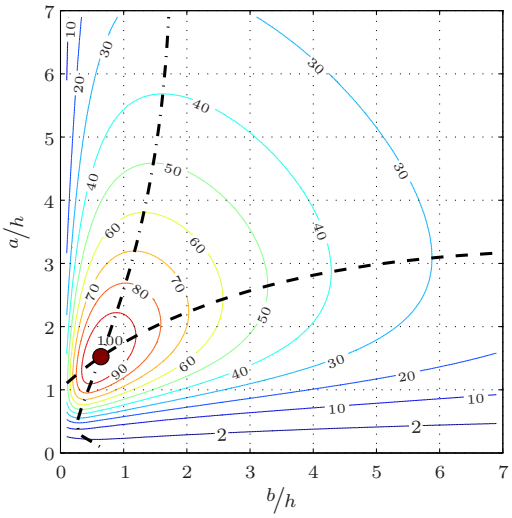

Figure 10: Normalized radial stiffness with respect to $\hat{\bar{k}}_r^A$ for n=5 of a repulsive type stacked bearing as function of a/h and b/h in %.

3.3 Halbach stacking

If now the magnetization is rotated by $\Delta\alpha = \pi/2$, instead of $\Delta\alpha = \pi$ as done for standard stacking, we get a "rotating magnetization", as Yonnet called it [2]. Such a configuration is shown in Figure 11 and is often referred to as Halbach stacking or Halbach array [14]. Similar to (24) an equation for the total stiffness can be stated

$$\bar{k}_r^n = n \cdot \bar{k}_r(0,0) + \sum_{i=1}^{n-1} 2 \cdot (n-i) \cdot \bar{k}_r(i \cdot a, -i \cdot \frac{\pi}{2}) \ . \tag{25}$$

To compare a Halbach array configuration with a standard stacked configuration the number of poles p is

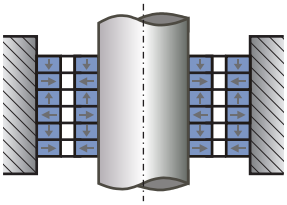

Figure 11: Stacked structure with rotating magnetization and $n = 6,\ p = 3$.

introduced. Looking at the field progression of the named configurations, Figure 12, it can be seen that for standard stacked bearings the number of poles is equal to the stacking number, $p = n_{Strd.}$, whereas for a Halbach configuration with $\Delta\alpha = \pi/2$ the number of poles which are formed are only half the number of stacked rings, $p = n_{Hlb.}/2$. The general relation between pole count, stacking number, a newly defined pole length l and rotation angle $\Delta\alpha$ is

$$p = n \cdot \frac{\Delta\alpha}{\pi} \quad , \quad l = \frac{\pi}{\Delta\alpha} \cdot a \ . \tag{26}$$

The result of the optimization is shown in Table 2, whereby (25) is used in (19) to get $\bar{k}_r^A$. Compared to the results for the standard stacking, Table 1, Table 2 is based on the number of poles p. But even when

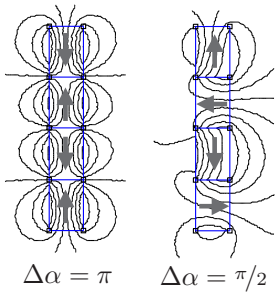

Figure 12: Field generated by one stacked ring, e.g. inner ring, with alternating (left) and rotating (right) magnetization and $n = 4$.

comparing same number of rings, the possible improvement for e.g. $n_{Strd.} = n_{Hlb.} = 2$ is 26%. The reason therefore is an even better coupling of e.g. first inner ring with second outer ring and so on, represented by the sum term of (25). Also note, that in column three of Table 2 the dimensionless polelength l/h instead of the dimensionless magnet heigth is given. As the pole length is twice the magnet heigth for this special case of $\Delta\alpha = \pi/2$, the desired magnet height a of each single ring is even smaller then for the standard stacked configuration. The sensitifity of a design with five poles is shown in Figure 13.

poles p ($\widehat{=} n_{Strd.}$)	stacking $n_{Hlb.}$	max. parameters: norm. pole length l/h	max. parameters: norm. magnet width b/h	max. value $\hat{\bar{k}}_r^A$	increase compared to $p = 1$ in %	increase to strd. stacking in %
1	2	1.686	0.661	0.09805	–	66.4
2	4	1.552	0.646	0.13841	41.2	77.6
3	6	1.562	0.639	0.15216	55.2	87.9
4	8	1.566	0.636	0.15870	61.9	91.2
5	10	1.566	0.634	0.16274	66.0	92.8
10	20	1.570	0.631	0.17072	74.1	95.5
20	40	1.570	0.630	0.17473	78.2	96.6

Table 2: Normalized, dimensionless radial stiffness for repulsive configurations with different numbers of Halbach stacked rings. Comparison to standard stacking relies on same number of poles!

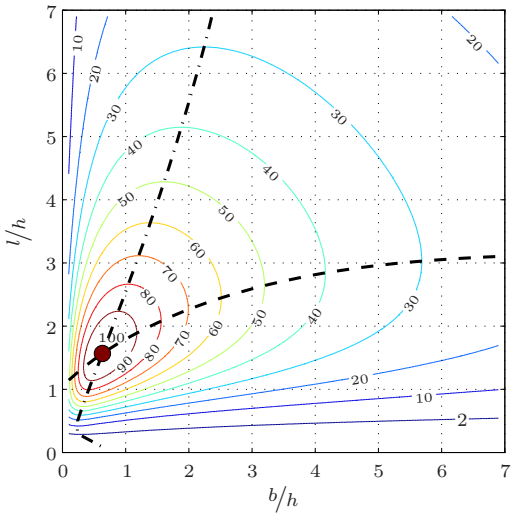

Figure 13: Normalized radial stiffness with respect to $\hat{\bar{k}}_r^A$ (n=10, p=5) of a repulsive type Halbach stacked bearing as function of the dimensionless parameters l/h and b/h in %.

3.4 Continuous rotating magnetization

The question is, what can be achieved when refining the rotation steps of the magnetization more and more, getting a continuous rotation as pictured in Figure 14? Therefore, the magnetization can be parameterized as follows:

$$\begin{aligned}\bar{\mathbf{M}}_1(z_1) &= M_1 \begin{bmatrix} \sin\left(\pi\frac{\bar{z}_1}{l}\right) \\ \cos\left(\pi\frac{\bar{z}_1}{l}\right) \end{bmatrix} \\ \bar{\mathbf{M}}_2(z_2) &= M_2 \begin{bmatrix} -\sin\left(\pi\frac{\bar{z}_2}{l}\right) \\ \cos\left(\pi\frac{\bar{z}_2}{l}\right) \end{bmatrix}\end{aligned} \tag{27}$$

In (27) the index $(\cdot)_1$ denotes a parameter of the inner ring and $(\cdot)_2$ one of the outer ring. Using (27)

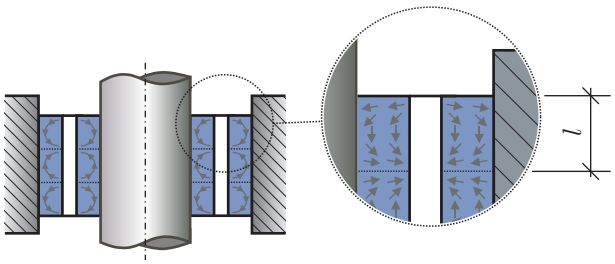

Figure 14: continuous rotating magnetization with $p = 3$.

when evaluating (15), an analytical expression for $\bar{k}_r$ can be found, nevertheless it is too long to be presented herein. With the parametrization (27) the resulting number of poles of $\bar{k}_r$ depends on the defined pole length l and the total magnet height, i.e. the integration limit in the $\bar{z}$ direction of (15).

The result of the optimization for best stiffness per magnet volume ratio is shown in Table 3 based on the number of poles. The sensitivity for p=1 and p=5 is shown in Figure 15.

Table 3: Normalized, dimensionless radial stiffness for repulsive configurations with continuous Halbach magnetization and different numbers of poles.

	max. parameters					
poles p	norm. pole length l/h	norm. magnet width b/h	max. value $\hat{\bar{k}}_r^A$	increase compared to $p = 1$ in %	increase to Halbach stacking in %	increase to strd. stacking in %
1	1.953	0.658	0.13062	–	33.2	121
2	1.644	0.647	0.17253	32.1	24.6	121
3	1.609	0.639	0.18878	44.5	24.1	133
4	1.598	0.636	0.19659	50.5	23.9	136
5	1.591	0.635	0.20139	54.2	23.7	138
10	1.580	0.631	0.21091	61.5	23.5	141
20	1.575	0.630	0.21569	65.1	23.4	142

3.5 Final comparison

To compare all configurations against each other, for standard stacking, Halbach stacking and for continuous Halbach magnetization the maximal value for the normalized stiffness per length is visualized in Figure 16.

4 Conclusion and Outlook

The presented investigations show, that between an optimized single ring bearing with homogeneous magnetization and an optimized contiguous Halbach magnetized system with several poles the stiffness per magnet volume ratio can be improved by a factor of about four, or in terms of business, the costs could be reduced to a quarter. Of course, this statement is more from a theoretical point of view, because it often might be hard to realize the optimal geometries. Nevertheless, by means of the given tables and figures, a system as close as possible to the optimal design can be achieved.

Another aspect that might be investigated more in detail concerns the magnetization procedure of magnets with continuous Halbach magnetization.

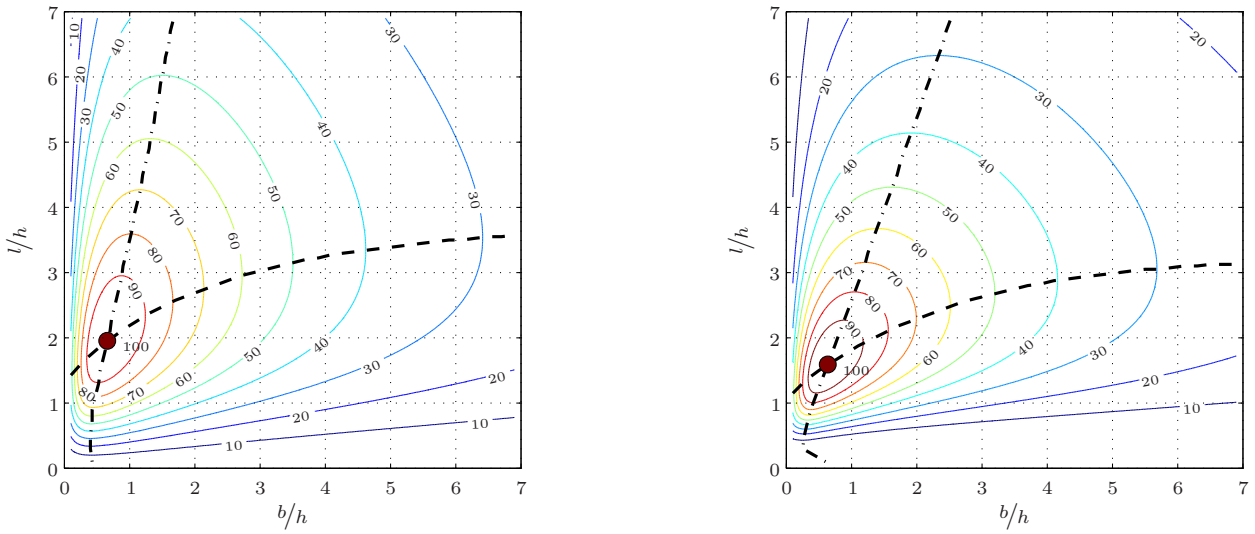

(a) p=1 (b) p=5

Figure 15: Normalized radial stiffness with respect to $\hat{\bar{k}}_r^A$ of a repulsive type bearing with contiuous Halbach magnetization as function of the dimensionless parameters l/h and b/h in %.

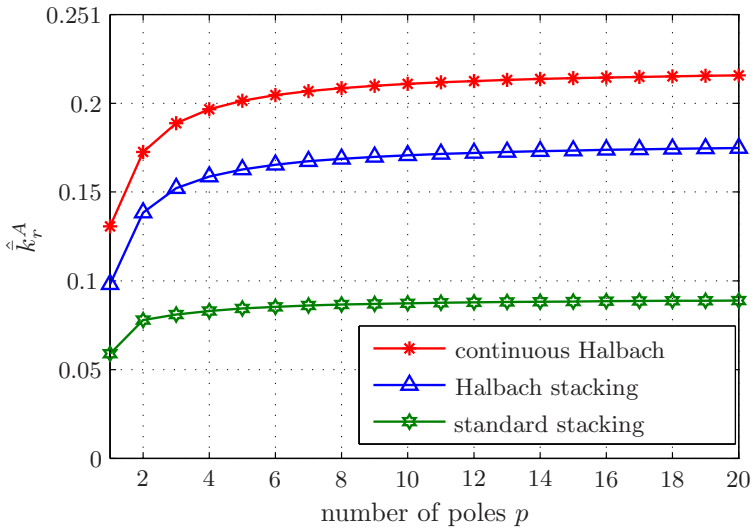

Figure 16: Comparison of the maximal normalized radial stiffness per length $\hat{\bar{k}}_r^A$ as function of the number of poles p

Even if all calculations where done for repulsive type bearings, all results can be transfered to attractive type configurations based on the full equivalence correlation

$$\bar{k}_{r,rep} = f(a, b, h, z_0, \alpha_1, \alpha_2) \Leftrightarrow \bar{k}_{r,att} = f(b, a, h, x_0, \alpha_1, -\alpha_2)$$

and the error considerations presented in the paper.

5 Acknowledgment

This work was conducted in the realm of the research program at the Austrian Center of Competence in Mechatronics (ACCM), which is a part of the COMET K2 program of the Austrian government. The authors thank the Austrian and Upper Austrian government for their support.

References

[1] Matthias Lang and J. K. Fremerey. Optimization of permanent-magnet bearings. In *6th International Symposium on Magnetic Suspension Technology*, Turin, Italy, October 2001. Politecnico di Turino.

[2] Jean-Paul Yonnet, Guy Lemarquand, Sophie Hemmerlin and Elisabeth Olivier-Rulliere. Stacked structures of passive magnetic bearings. *Journal of Applied Physics*, 70(10):6633–6635, November 1991.

[3] Max Baermann. Magntische Lagerung, German Patent No. DE 1017871B, April 1965.

[4] Jean-Paul Yonnet. Analytical calculations of magnetic bearings. In *Proceedings of the fifth International Workshop on rare Earth-Cobalt Permanent Magnets and their Applications*, pages 199–216, Roanoke, Virgiia (U.S.A.), June 1981.

[5] E. P. Furlani. A formula for the levitation force between magnetic disks. *IEEE Transactions on Magnetics*, 29(6):4165–4169, November 1993.

[6] R. Ravaud, G. Lemarquand and V. Lemarquand. Force and stiffness of passive magnetic bearings using permanent magnets. part 1: Axial magnetization. *IEEE Transactions on Magnetics*, 45:2996–3002, 2009.

[7] R. Ravaud, G. Lemarquand, and V. Lemarquand. Force and stiffness of passive magnetic bearings using permanent magnets. part 2: Radial magnetization. *IEEE Transactions on Magnetics*, 45:3334–3342, 2009.

[8] Matthias Lang. Fast calculation method for the forces and stiffnesses of permanent-magnet bearings. In *8th International Symposium on Magnetic Bearings*, pages 533–538, Mito, Japan, August 2002. Ibaraki University.

[9] Jean-Paul Yonnet. Permanent magnet bearings and couplings. *IEEE Transactions on Magnetics*, 17(No. 1):1169–1173, January 1981.

[10] Gerald Jungmayr, Wolfgang Amrhein, Walter Angelis, Sigfried Silber, Herbert Grabner and Dietmar Andessner. Design of a hybrid magnetic bearing. In *8th International Symposium on Magnetic Suspension Technology*, Dresden, Germany, 2005.

[11] Matthias Lang. *Berechnung und Optimierung von passiven permanentmagnetischen Lagern für rotierende Maschinen*. PhD thesis, Technische Universität Berlin, Berlin, July 2003.

[12] Walter Greiner. *Klassische Elektrodynamik*. Theoretische Physik. Harri Deutsch, 7., überarbeitete auflage edition, 2008.

[13] Gerald Jungmayr. *Der magnetisch gelagerte Lüfter*. PhD thesis, Johannes Kepler Universität Linz, 2008.

[14] Kevin D. Bachovchin, James F. Hoburg and Richard F. Post Magnetic Fields and Forces in Permanent Magnet Levitated Bearings. *IEEE Transactions on Magnetics*, accepted for publication.